An ozone depletion event in the sub-arctic surface layer over Hudson Bay, Canada

**B. A. Ridley · T. Zeng · Y. Wang · E. L. Atlas ·
E. V. Browell · P. G. Hess · J. J. Orlando ·
K. Chance · A. Richter**

Abstract During the Tropospheric Ozone Production about the Spring Equinox (TOPSE) program, aircraft flights during April 7–11, 2000 revealed a large area air mass capped below ~500 m altitude over Hudson Bay, Canada in which ozone was reduced from normal levels of 30–40 ppbv to as low as 0.5 ppbv. From some of the in-situ aircraft measurements, back-trajectory calculations, the tropospheric column of BrO derived from GOME satellite measurements, and results from a regional model, we conclude that the event did not originate from triggering of reactive halogen release in the sub-Arctic region of Hudson Bay but resulted from such an event occurring at higher latitudes over the islands of the northern Canada Archipelago and nearby Arctic Ocean with subsequent transport over a distance of 1,000–1,500 km to Hudson Bay. BrO_x remained active during this transport despite considerable changes in the conditions of the underlying surface suggesting that chemical recycling during transport dominated any local halogen input from the surface. If all of the tropospheric column density of BrO is distributed uniformly within the surface layer, then the mixing ratio of BrO derived from the satellite measurements is at least a factor of 2–3 larger than derived indirectly from in situ aircraft measurements of the NO/NO_2 ratio.

B. A. Ridley (✉) · P. G. Hess · J. J. Orlando
Atmospheric Chemistry Division, NCAR, P. O. Box 3000, Boulder, CO 80307, USA
e-mail: ridley@ucar.edu

T. Zeng · Y. Wang
School of Earth and Atmospheric Sciences, Georgia Institute of Technology, Atlanta, GA 30332, USA

E. L. Atlas
Rosenstiel School of Marine and Atmospheric Science, University of Miami, Miami, FL 33149, USA

E. V. Browell
Atmospheric Sciences, NASA Langley Research Center, Hampton, VA 23681, USA

K. Chance
Harvard-Smithsonian Center for Astrophysics, Cambridge, MA 02138, USA

A. Richter
Institute of Environmental Physics, University of Bremen, P. O. Box 330 440, 28334 Bremen, Germany

1 Introduction

Numerous investigations of near-complete destruction of ozone in the Arctic surface layer in spring have been made since its discovery almost two decades ago from observations made at Alert, Nunavut, Canada (Bottenheim et al. 1986) and Point Barrow, Alaska (Oltmans and Komhyr 1986). Much of the current understanding of the processes involved in the ozone destruction has been summarized by Barrie and Platt (1997), Barrie et al. (1998), and by manuscripts describing results from recent intensives conducted at Alert and Summit, Greenland, in spring 2000 that have been published in a special section of Atmospheric Environment (36, 2467–2797, 2002). Although both reactive chlorine and bromine are involved in the catalytic destruction of ozone, reactions involving bromine dominate (Le Bras and Platt 1995; Foster et al. 2001; Spicer et al. 2002). The active bromine is considered to ultimately derive from sea salt bromide (Platt and Moortgat 1999), but the process that triggers the release of active bromine has yet to be identified conclusively (Bottenheim et al. 2002). The role of frost flowers remains controversial: Rankin et al. (2002), Kaleschke et al. (2004), Jacobi et al. (2006), and Sander et al. (2006) favor them as an important direct source while Simpson et al. (2005, 2006), Domine et al. (2005) and Kalnajs and Avallone (2006) present arguments that frost flowers do not play a unique role in directly triggering reactive halogen release to the atmosphere.

Two catalytic cycles are believed to dominate the net ozone destruction: $2O_3 \rightarrow 3O_2$ (Le Bras and Platt 1995; Platt and Lehrer 1997; Wagner et al. 2001). The first cycle includes reactions 1–3, where reaction 3 is usually rate limiting, which yields a quadratic dependence of the ozone loss rate on BrO.

$$Br_2 + h\nu \rightarrow 2Br \tag{1}$$

$$2(Br + O_3 \rightarrow BrO + O_2) \tag{2}$$

$$BrO + BrO \rightarrow 2Br + O_2 \tag{3}$$

The second cycle is reaction 2 followed by reactions 4–6. Here reaction 4 is usually rate limiting, which yields a linear dependence of the ozone loss rate on BrO. Reactions of OH with methane or other hydrocarbons that lead to production of HO_2 could supplement reaction 6.

$$Br + O_3 \rightarrow BrO + O_2 \tag{2}$$

$$BrO + HO_2 \rightarrow HOBr + O_2 \tag{4}$$

$$HOBr + h\nu \rightarrow Br + OH \tag{5}$$

$$OH + CO(+O_2) \rightarrow HO_2 + CO_2 \tag{6}$$

The efficiency of either catalytic cycle of course depends on the rate of conversion of active BrO_x (Br + BrO) to non-radical constituents. Reaction of Br with formaldehyde or

higher carbonyls (Sumner and Shepson 1999) and ethyne (Jobson et al. 1994) form reservoir HBr, which can be deposited to the surface or to aerosols to provide a source of bromide (Br^-) in addition to that from sea-salt. Reaction of BrO with NO_2 forms $BrONO_2$ that can be hydrolyzed on the surface ice/snow or on aerosols to yield HOBr and HNO_3 in the aqueous phase (Hanson and Ravishankara 1995). HOBr formed in reaction 4 is also readily deposited to surfaces.

Currently, recycling of BrO to the gas phase is believed to result from reaction 7, which occurs with uptake of gaseous HOBr, within or on the acidic snow/ice surface or on aerosols (McConnell et al. 1992; Fan and Jacob 1992; Tang and McConnell 1996).

$$HOBr(aq) + H^+(aq) + Br^-(aq) \rightarrow Br_2(aq) + H_2O \qquad (7)$$
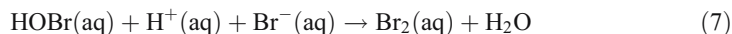
Aqueous (aq) Br_2 is readily released to the gas phase and undergoes rapid photolysis during daytime, reaction 1. It is reaction 7, where a single Br atom that enters the surface or aerosol leads to release of up to two gas phase atoms, that yields the "bromine explosion" described by Platt and Lehrer (1997). Reaction of HOBr with chloride in the aqueous phase can also produce BrCl that is readily photolysed once in the gas phase.

During the Tropospheric Ozone Production about the Spring Equinox (TOPSE) C130 aircraft program (Atlas et al. 2003), a large area air mass in which ozone was reduced from typical background levels of 30–40 ppbv to as low as 0.5 ppbv was found in a shallow surface layer over Hudson Bay, Canada, on flights of April 7, 10, and 11, 2000. The broad features of the event, determined from an on-board lidar and in-situ O_3 instrument, are described in Section 2. Back-trajectories, the behavior of tropospheric column densities of BrO derived from satellite data, and a regional model are used in Section 3 to argue that the ozone loss was not triggered by halogen activity local to the Hudson Bay surface layer. In Section 4, other measurements made from the aircraft are used to provide further details of the event and an indirect comparison of the BrO abundance, which was not measured from the aircraft, with that derived from satellite retrievals. Implications from the aircraft and satellite observations are summarized in Section 5.

2 Remote sounding and in situ observations of the ozone depletion event (ODE)

A map of the Arctic region showing locations that are referred to in the discussion is given in Fig. 1. The ODE over the Hudson Bay region was first detected by the UV Differential Absorption Lidar system (UV DIAL; Browell et al. 2003) during a flight on April 7, 2000 from Thule Air Base, Greenland (76.5°N, 68.8°W) to Churchill, Manitoba (58.8°N, 94.2°W). Figure 2 shows the flight track and Fig. 3 gives the ozone distribution from DIAL above and below this track. The aircraft altitude is shown in detail on the lidar map and its color code is the same as that of the DIAL data but was derived from the in situ ozone instrument. DIAL shows a hint of low surface ozone starting near 70.2°N or when the aircraft was above the northwestern shore of Baffin Island but almost immediately low-level clouds blocked the lidar from seeing the surface layer. Less than 10 ppbv ozone was measured by the lidar starting near 1815 UT (1315 local time (LT) at Churchill) and continuing until the aircraft prepared for landing, or over a distance of ~600 km above the lowlands of and the western shore of Hudson Bay. It is quite possible that the ODE extended farther north to Baffin Island. The ODE was confined to a depth of less than 1 km above the surface but could not be examined with the in situ instruments because the aircraft had suffered a mechanical problem.

Fig. 1 Polar map showing loca-
tions that are referred to
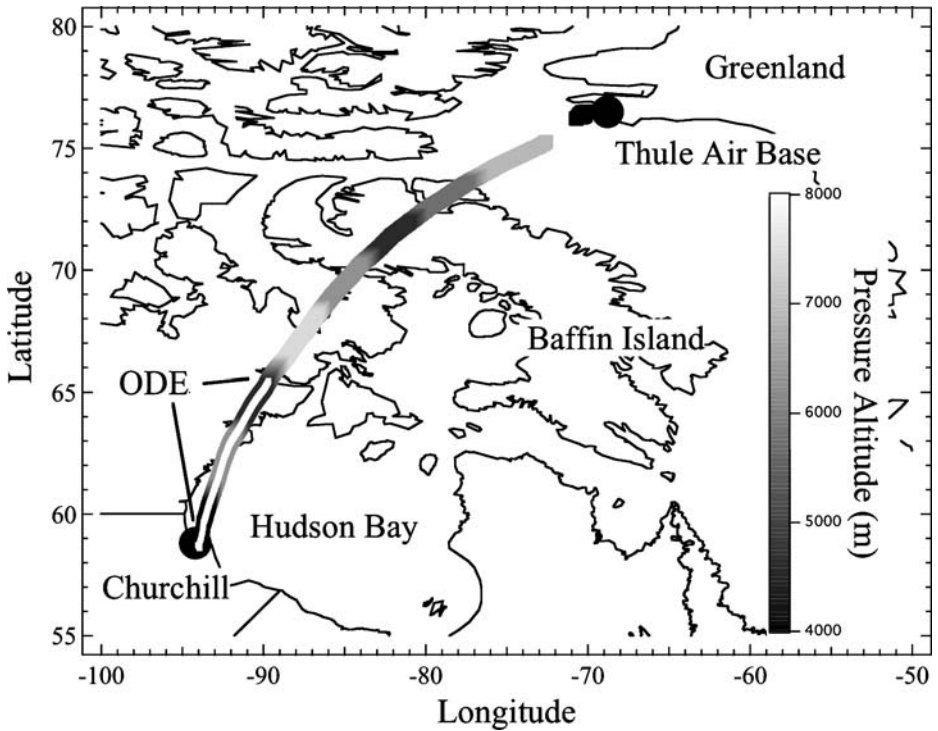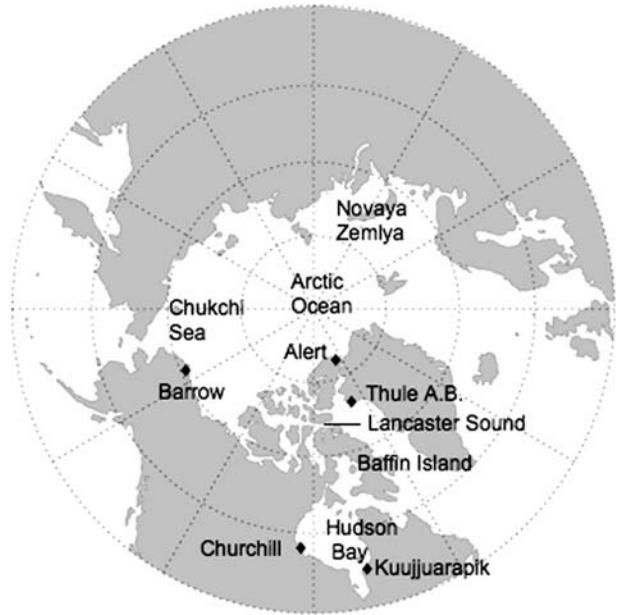in the text

Fig. 2 Track of the April 7 flight from Thule Air Base, Greenland to Churchill, Manitoba. The ODE was recorded by DIAL over the region indicated by the *white bar* within the flight track
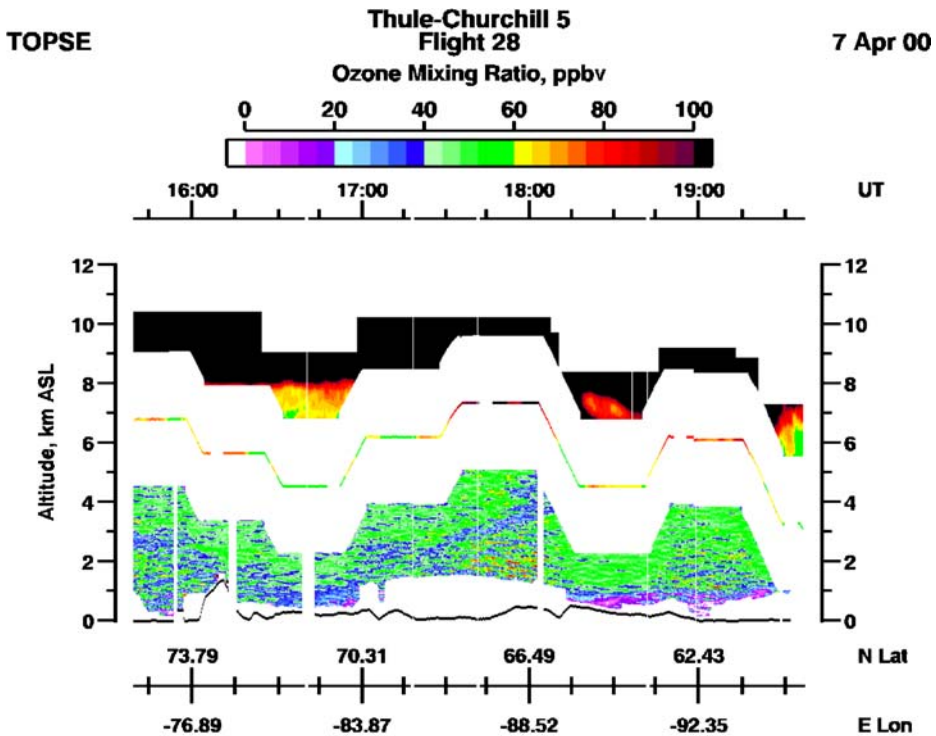
Fig. 3 The ozone distribution above and below the aircraft track from DIAL for April 7. The ODE is seen at low altitude toward the end of the flight, after ~1815 UT. There is a hint of the ODE starting near 70.2°N but low-level clouds almost immediately blocked the lidar

The next flight was not possible until April 10 when the aircraft first ascended to ~5 km altitude and traveled ENE toward central Hudson Bay to enable DIAL to search for any ODE. As shown in Fig. 4, and for reasons to be described later, the same ODE as observed on April 7 was detected starting near 1515 UT or when ~300 km ENE of Churchill. The ODE persisted below ~500 m altitude for ~250 km or as far as the aircraft flew on this track until it turned at 84°W and headed northwest. The ODE ended on this northwesterly track at 61.4°N, 87.6°W or when ~200 km north of the initial ENE track. Figure 5 shows that the ODE region was also accompanied by enhanced aerosol backscatter (by particles of 0.5–2 μm diameter). Near 62.5°N the aircraft reversed course and descended to investigate lower altitudes with the in situ instrumentation. After these low altitude investigations, the aircraft ascended to 4.6 km to return to Churchill. DIAL did not observe any significant change in the position of the western boundary of the ODE over the ~6 h period of the flight.

During the first descent to low altitudes, the in situ O_3 instrument also started to record the ODE at 61.4°N as the aircraft descended through 300–400 m altitude. Figure 6 shows the time series of in situ ozone, wind speed, and relative humidity with respect to ice for the flight starting from near the time of this first descent (D1). The C130 first flew at a constant altitude of 95 m for ~110 km (62,300–63,400 s in Fig. 6) where O_3 was only partially depleted and variable. Median and mean O_3 were 6.3 and 7.2 (±2.5) ppbv, respectively. The aircraft then descended to 30 m altitude and continued southeast for another ~110 km where O_3 became more uniform and mixing ratios decreased below 1 ppbv. Between 66,300 and 70,400 s, the aircraft made four east–west stacked flight legs of ~100 km
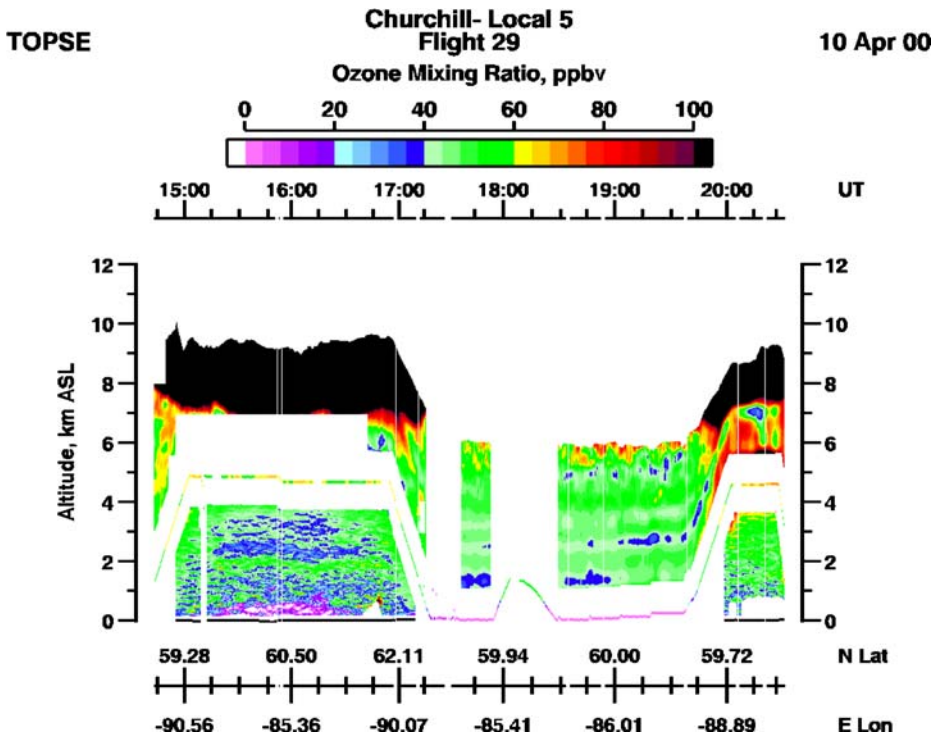
Fig. 4 Ozone distribution above and below the aircraft track for April 10 from the lidar. The ODE was recorded between 1515 and 1615 UT below ~500 m altitude. It was not seen by DIAL on the return to Churchill, after 1945 UT because the aircraft was just to the west of the ODE boundary by the time the downward-looking lidar could operate

distance at 30, 95, 150, and 270 m. Over this 68 min period of sampling ozone was remarkably uniform and low: minimum 0.47, maximum 1.41, median 0.70, and mean 0.74 (±0.14) ppbv over 3,522 (1 s) samples. Winds were light at 1–3 m/s, from the west to northwest sector, which supports the proposal that this ODE was the same one as observed on April 7. The surface layer was also near saturation relative to ice. The vertical structure of the ODE is shown in Figs. 7 and 8 for the four soundings that are labeled in Fig. 6. As has been observed routinely (Leaitch et al. 1994; Ridley et al. 2003), the ODE was capped by a moderate to weak temperature inversion or below 440–490 m in the southern region, and below 320 m on the northwestern edge of the ODE. The last ascent (A2) was near the western edge of the ODE and the multiple sharp gradients in ozone in the 500–1,000 m altitude region hint of exchange and mixing across the inversion layer.

The ODE persisted in the region until at least the next morning. On April 11, the aircraft returned to its home base in Broomfield, Colorado starting near 0900 LT, but the first half hour of the flight was used to fly low altitude legs at 525 and 30 m altitude due east of Churchill. Low O_3 was detected at both low altitudes immediately after the in situ instrument started operating after take-off and for a distance of ~180 km until the C130 climbed and turned heading to the southwest. Both the DIAL ozone and back-scatter (Fig. 9a, b) and in situ (Fig. 10) ozone instruments revealed the ODE extended to the farthest eastern point of the flight track over Hudson Bay and from DIAL also overland to ~25 km west and ~260 km south of Churchill. Compared to the previous flight, the ODE
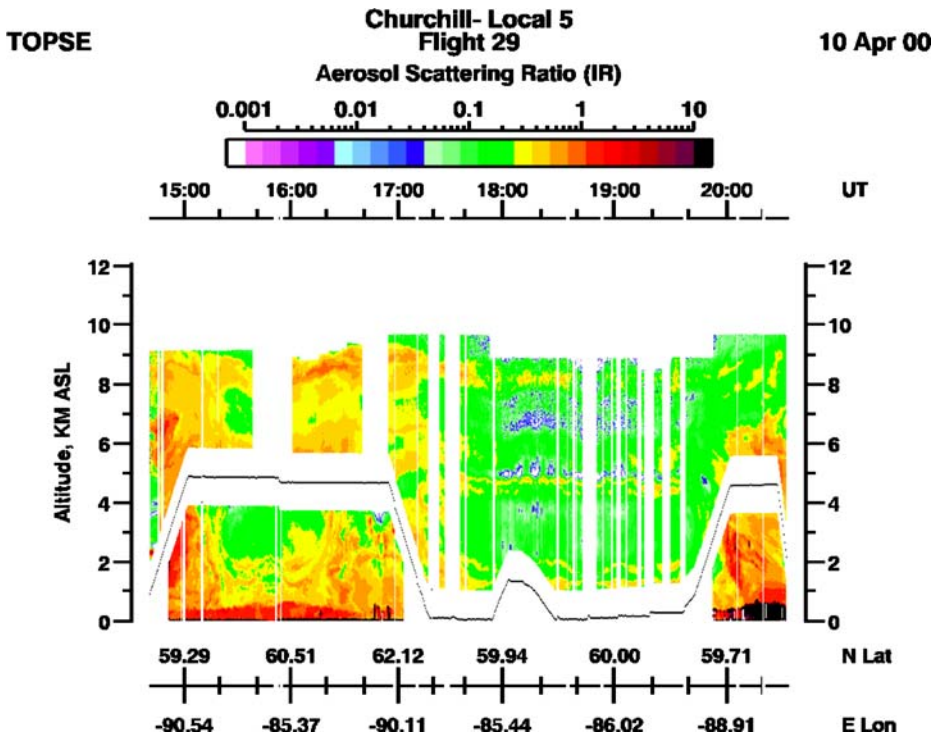
Fig. 5 DIAL aerosol scattering ratio for April 10. The region of the ODE of Fig. 4 also corresponds to higher backscatter due to particles in the size range of 0.5–2 μm diameter

extended to a slightly higher altitude (550 m versus 440–490 m) and O_3 within the ODE was significantly elevated (Fig. 11) even at the lowest flight altitude. Minimum, maximum, median and mean O_3 during the ∼30 min of flight at 525 and 30 m were 3.7, 12.3, 10.2, and 9.6 (±1.7) ppbv. There was also considerable structure in the O_3 profile (Fig. 11) from 600–800 m indicative of some exchange across the inversion due to significantly larger wind speeds although there was no shear in either speed or direction (winds were from the NW, 290–310°, over the altitude range of Fig. 11). With the substantial increase in wind speed from the afternoon of April 10 to the morning of April 11, different portions of the ODE were sampled on the two flights.

From the start of the TOPSE program on Feb. 7, 2000 to the flight of April 7, no ODEs were detected over the Hudson Bay region during 11 flight legs within the surface layer or by DIAL on overpasses at higher altitude (Ridley et al. 2003). On a flight from Churchill to Thule on April 4, DIAL did not detect any ODE over the western portion of Hudson Bay although surface conditions, insolation and surface layer meteorology were not dramatically different from conditions only 3 days later. Thus detection of the ODE on April 7 was unexpected and we initially assumed that ODE processing was somehow triggered locally over the sub-arctic frozen and mostly snow-covered salt-water of Hudson Bay. Apart from some sunlight throughout the winter period at the latitude of mid-Hudson Bay, the conditions there were similar to those of the Arctic Ocean region where ODEs are frequently triggered after the return of sunlight in spring. For example, Richter et al. (1998) and Kaleschke et al. (2004) interpreted GOME satellite observations of enhanced total
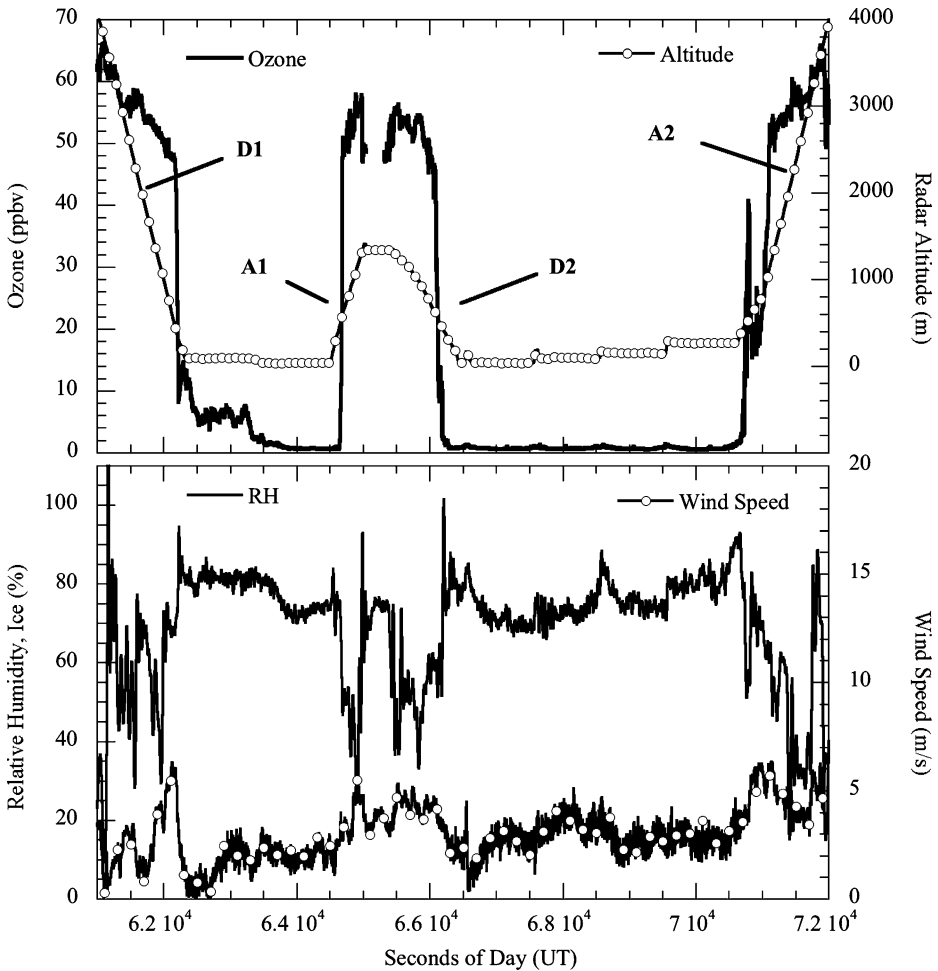
Fig. 6 Time series of 1-s data for the lower altitude flight legs of April 10. *A1*, *A2*, *D1*, *D2* mark the first and second ascent/descent from/to the surface layer

column BrO to conclude that there must be large local sources that trigger active bromine release in the Hudson Bay region. The analysis presented in the next section, however, argues that this particular ODE was imported to the Hudson Bay region from higher latitudes rather than being the result of local triggering of halogen activity, a possibility that was not considered by Richter et al. (1998) or Kaleschke et al. (2004). Long-range transport of ODEs within the Arctic Ocean region is well known: ODEs recorded at the Pt. Barrow and Alert ozone monitoring stations (see Fig. 1), for example, are predominantly the result of transport from development regions over the Arctic Ocean. Indeed, we are unaware of detailed measurements made during the triggering-phase of halogen activation and the initial ozone destruction. Ridley et al. (2003) have also given examples of ODEs observed on other TOPSE flights that were the result of transport well south of their origin over the Arctic Ocean region. Other observations from GOME and calculated air mass trajectories also suggested transport to Hudson Bay in the second week of March 2000, but the TOPSE flights did not overlap with this period. Thus, this earlier episode is not discussed here.

Fig. 7 April 10 altitude profiles of ozone during the ascents (*A1*, *A2*) and descents (*D1*, *D2*) labeled in Fig. 6. D1 was a slant descent as the aircraft headed southeast. The other ascents and descent were near vertical. Data are 1-s
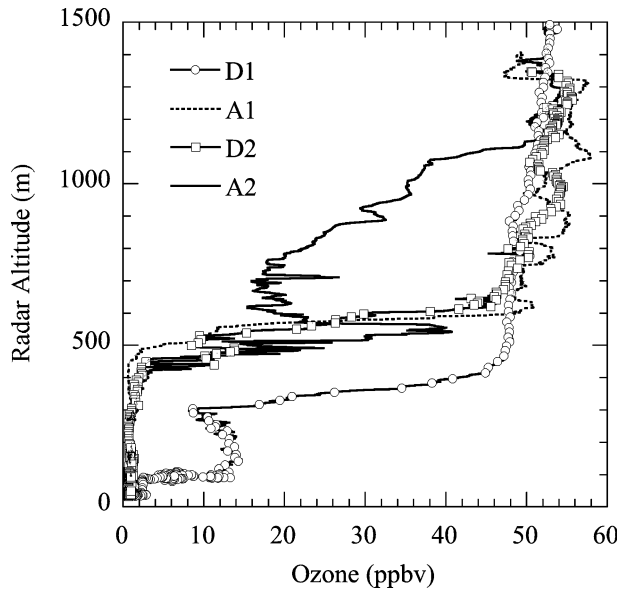
3 Air mass trajectories, GOME tropospheric column densities, and polar regional modeling

Figure 12 presents 10-day back-trajectories from the locations of the April 10 flight track where in-situ ozone was measured to be less than 10 ppbv or from altitudes mostly below 450 m altitude. These trajectories were calculated based on assimilated meteorological fields using the polar version of the Penn State/National Center for Atmospheric Research

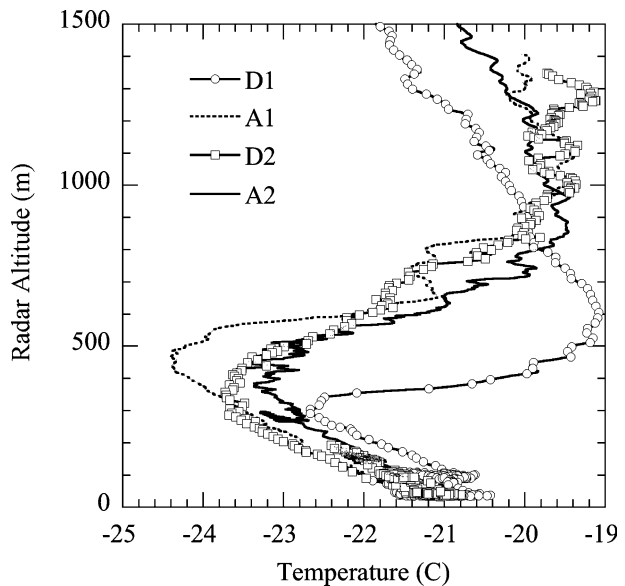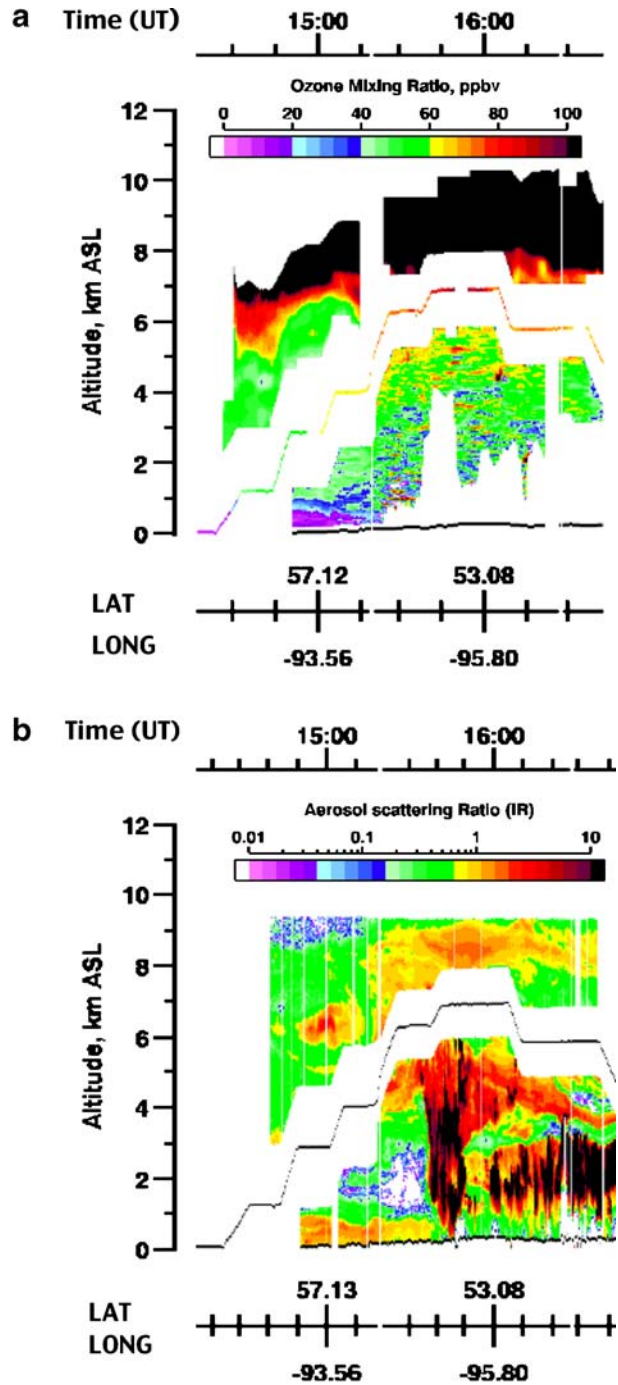**Fig. 8** Temperature profiles corresponding to the soundings of Fig. 7

Fig. 9 a DIAL ozone distribution for the first part of the April 11 flight. **b** DIAL aerosol scattering ratio for the first part of the April 11 flight
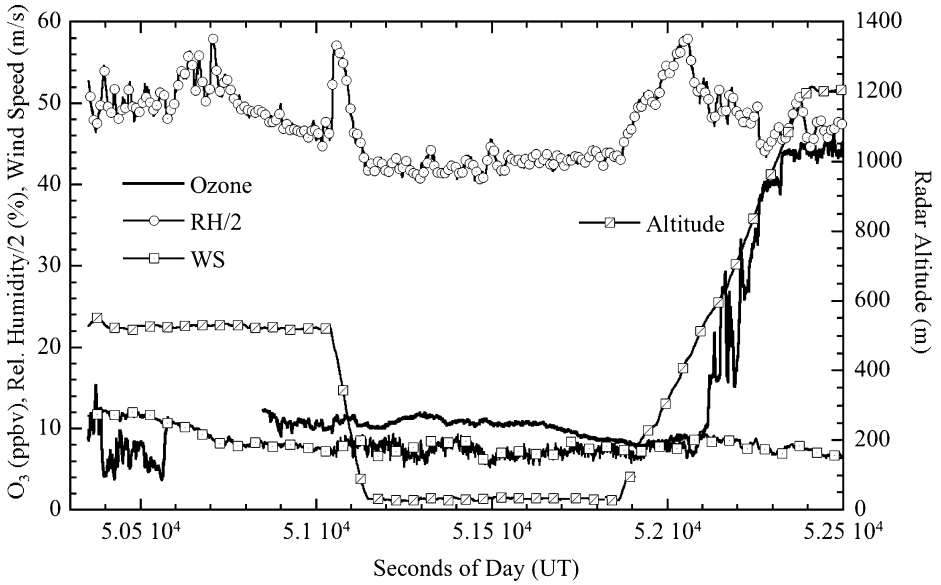
Fig. 10 Time series of 1-s data for the lower altitude flight legs of April 11 as the aircraft flew due east of Churchill
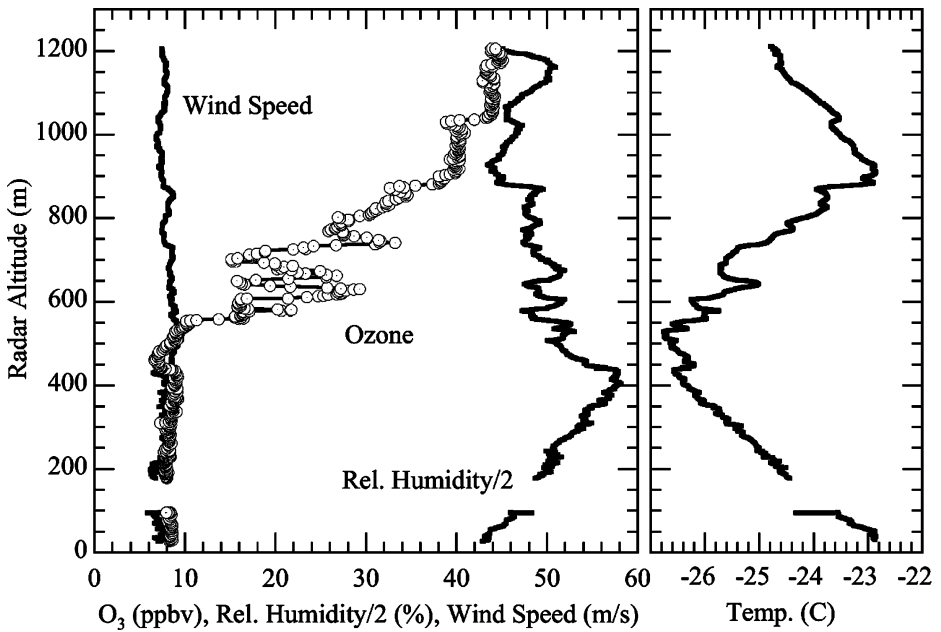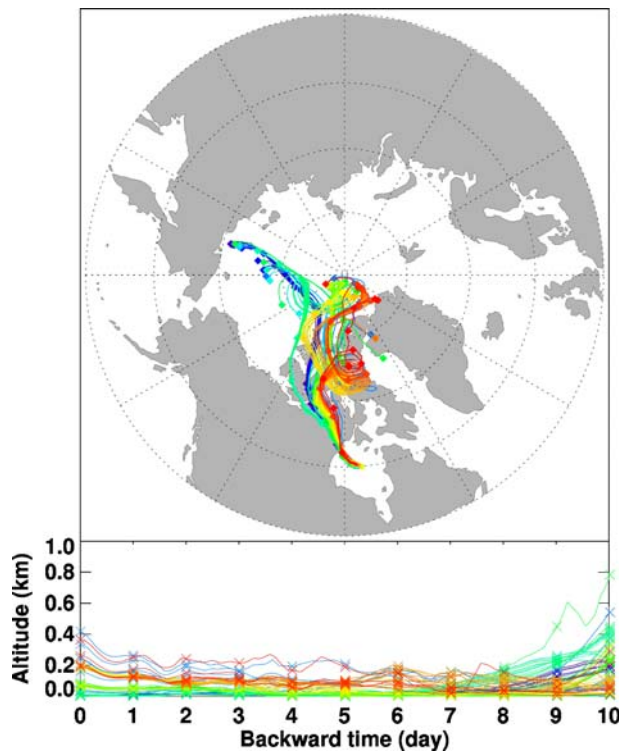

Fig. 11 Ascent profiles of ozone, wind speed, relative humidity and temperature recorded near 51,900 μs of Fig. 10, or when farthest east of Churchill

Fig. 12 10-day back-trajectories from the track of the April 10 flight where the ozone mixing ratio was less than 10 ppbv or for altitudes below ~500 m

(NCAR) meso-scale model MM5 (Zeng et al. 2006). This kinematic trajectory calculation is similar to that by Fuelberg et al. (1996); self-adjusting time step and higher-order time integration are added to improve the calculation (Arimoto et al. 2007). The trajectories, which remain at low altitudes, show air mass transit over the many islands of the northern Canada Archipelago, one group having 10-day origins over the Arctic Ocean near the North Pole and another group having 10-day origins off the coast of Siberia. Most of the trajectories within the group with 10-day origins near the pole spent an approximately 3-day period circumventing a region over and west of Baffin Island. Transit from this region to central Hudson Bay required 4–6 days. Trajectories (not shown) from the 1 and 2 km altitudes of the flight track remained for the entire previous 10 days over a small region from the northern coast of Hudson Bay to 70°N and between the western shore of Baffin Island and 110°W, i.e., over an area roughly equivalent to that of the circular surface layer trajectories of Fig. 12, but shifted about 8° farther south. Although the accuracy of surface layer trajectories is always a concern, confidence in them is gained by also determining NOAA HYSPLIT trajectories (not shown) from the flight track for altitudes below 500 m. Essentially the same pattern as given in Fig. 12 was obtained with some trajectories reproducing the circular pattern of Fig. 12 but with more of the 10-day trajectories extending to near the coast of Siberia between 125°E and 180°E. Trajectories for April 6–12 were basically similar to those of Fig. 12: all indicated 4–5 day origins from over the Archipelago and 10-day origins from over the Arctic Ocean with some extending to northern Siberia. On April 5 and 6, most of the 10-day trajectories remained over the Archipelago region with only a few extending to the open ocean to the north.

The trajectories of course cannot indicate where halogen activation initiated. Figure 13 gives a time series of the tropospheric vertical column density (TVCD) of BrO derived
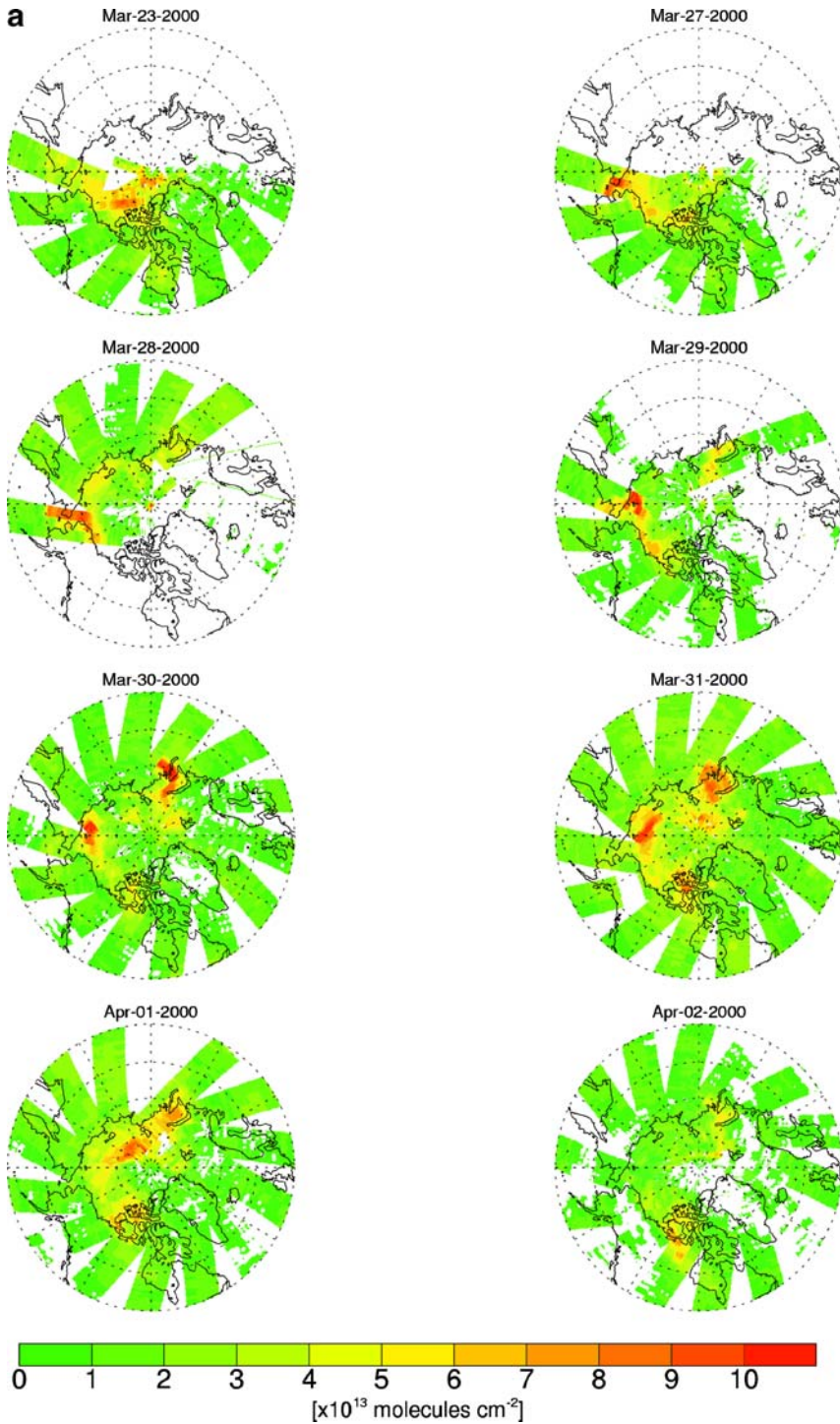
Fig. 13 A series of polar maps showing the tropospheric column density of BrO derived from the GOME satellite instrument. **a** March 23–April 2, **b** April 3–11
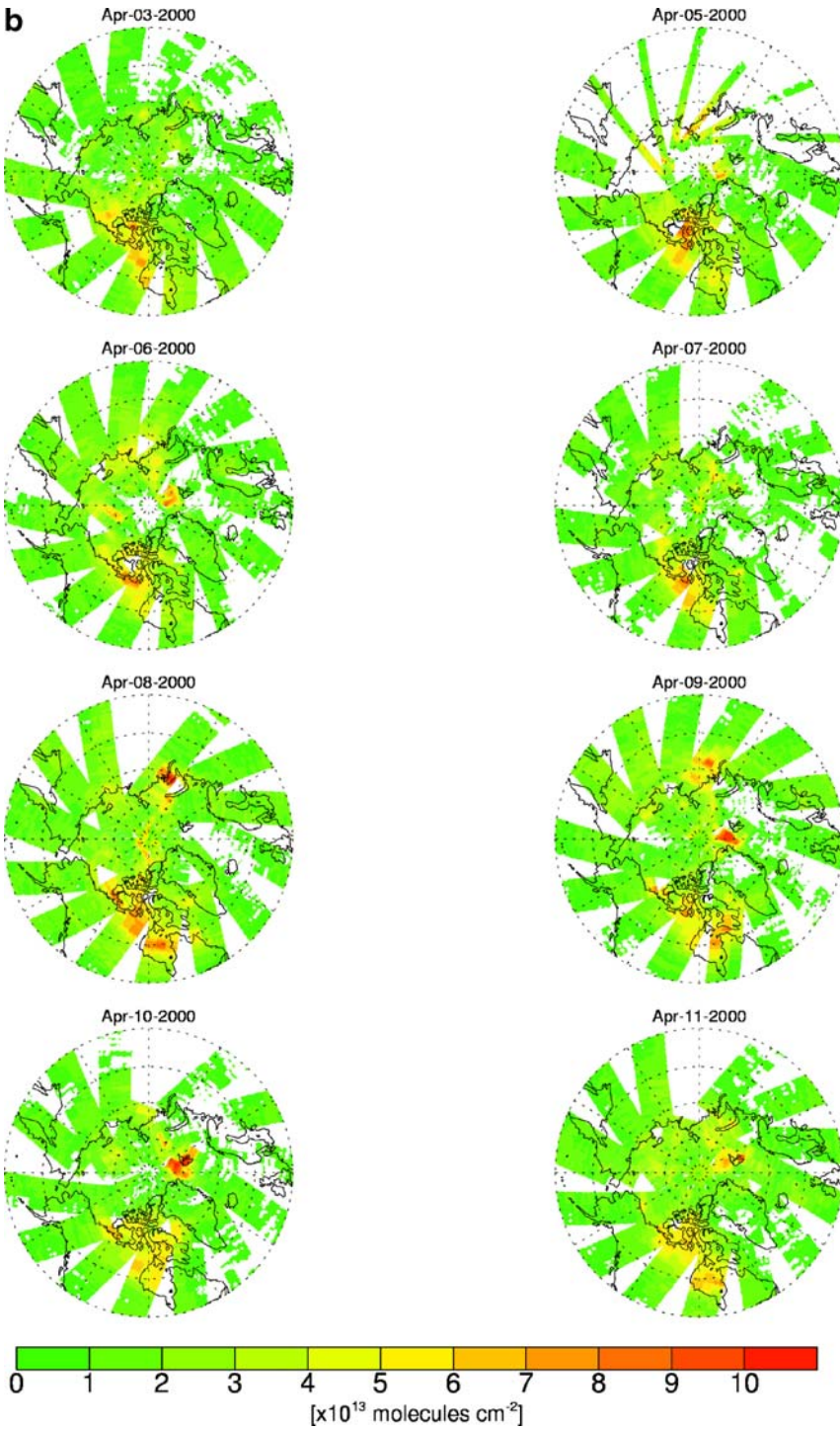
Fig. 13 (Continued)

using the procedure described by Zeng et al. (2003) from the total atmosphere (troposphere + stratosphere) column density measured by the Global Ozone Monitoring Experiment (GOME) instrument on board the European research satellite ERS-2 (Richter et al. 1998; Wagner and Platt 1998; Frieß et al. 2004). Uncertainty in the TVCD from spectral fitting of GOME measurements is estimated to be ~24% in April. We estimate the stratospheric vertical column uncertainty by computing its standard deviation, which is 6% in April. The air mass factor (AMF) is not sensitive to the specified BrO thickness from 0.3 to 1 km. The surface albedo change from spring to summer in the region is about 0.1 (Wang and Key 2005), which we use to calculate an uncertainty of 20% in the AMF. We choose to use the full range of albedo change from spring to summer because of a lack of measurements of near-UV aerosol optical depth in the Arctic region. Assuming that all of these uncertainties are uncorrelated, the overall uncertainty in the TVCD is estimated as the square root of the sum of individual errors squared or 40%.

The time series is extended back to March 23, well before the start of the 10-day trajectories to the April 10 flight track over Hudson Bay, to allow comparison of the changes in BrO in the Arctic region with other TOPSE observations. If it is assumed that the TVCD is completely located within the near-surface layer, below ~500 m, then orange to red regions (TVCD $\sim 10 \times 10^{13}$ molec cm^{-2}) of Fig. 13 correspond to a BrO mixing ratio uniformly distributed within this layer of ~75 pptv. Such a large mixing ratio would lead to very large ozone destruction rates of ~5 ppbv/h (Tuckermann et al. 1997). Thus, although elevated BrO does not have to imply immediate ozone depletion, such an air mass even of age less than a day would suffer easily measured ozone reduction from the typical background levels of 20–25 ppbv that are observed in spring at Barrow or from levels of 30–40 ppbv observed at Alert. Modulation of the TVCD can occur by changes in BrO$_x$ source and removal processes or changes in the BrO/Br ratio for constant BrO$_x$. Apparent modulation could also occur through low-level cloud formation or removal. Conversely, an ODE could occur without elevated BrO$_x$ if the air mass had insufficient time to recover from previous halogen activation by mixing processes.

With the large surface layer mixing ratios implied by the orange-red areas of Fig. 13, a close correspondence would be expected with ozone depletion events. Fig. 13b shows that elevated TVCDs were present over Hudson Bay during the time of the aircraft observations of depleted ozone from April 7–11. Indeed, the high BrO remained over Hudson Bay until April 14–15 when the region of elevated TVCD moved eastward and decreased in intensity. On April 10, the area of high BrO extended much farther north than the ~61° northern boundary of the ODE determined by DIAL, and the high BrO had persisted north of 65°N (the top of Hudson Bay) for 3–4 days, long enough for significant ozone depletion. The difference in the northern extent of high BrO and low O$_3$ is unclear because GOME has good N–S resolution (40 km) but poorer E–W resolution (320 km). It is possible that the aircraft simply flew over horizontal structure in the ODE that only suggested a northern boundary.

There are other examples where the aircraft observations of an ODE in the surface layer occurred in concert with elevated TVCDs. The March 23 panel of Fig. 13a shows a large area of elevated TVCD over the Arctic Ocean. Large BrO had not existed north of Alert for more than 1–2 days, but significant ozone reduction was observed over a distance of 220 km during a TOPSE flight leg at 30 m altitude over the Lincoln Sea/Arctic Ocean north of Alert. Ozone was as low as 0.03 ppbv (Ridley et al. 2003). The March 31 to April 5 panels of Fig. 13 show that large TVCDs were present over the Canadian Archipelago. On April 4, during a TOPSE flight from Churchill to Thule, DIAL was blocked by low level clouds from ~66 to ~70°N, but observed a small region of surface depleted ozone near 71°N

or just west of Baffin Island. Also a 30 m altitude flight leg of ~100 km distance over the western portion of Lancaster Sound (see Fig. 1) in the Archipelago region revealed significant ozone reduction from 30–40 ppbv to 12 ppbv.

During the period March 27–31, Fig. 13a shows strong BrO activation over three regions of the Arctic Ocean: over the Chukchi Sea north of Alaska and Siberia; north of Russia near the Island of Novaya Zemlya; and over the Canadian Archipelago chiefly west of Baffin Island where surface elevations are as high as 2.4 km on its northern half. In spring 2000, elevated TVCDs appeared to initiate most frequently but not exclusively over these three areas. Although some of the April 10 (indeed for the period April 6–April 16) back-trajectories extended from Hudson Bay to the BrO development north of Siberia, it is unlikely that this region was the major source of the activation that resulted in the depleted ozone observed by the aircraft over Hudson Bay from April 7–11. Elevated BrO does not follow these trajectory tracks across the Arctic Ocean but rather expands and transits along the coast north of Alaska and western Canada. It is possible that ozone depletion did occur in the region of BrO activation identified by GOME north of Siberia but that BrO_x was removed as the surface layer air mass transited across the Arctic Ocean and south to Hudson Bay. However, it is more likely that the initial triggering of the BrO activation responsible for the Hudson Bay ODE occurred in the Archipelago region. This source is consistent with some of the April 10 trajectories being rather stagnant over this region for several days (those trajectories following the circular path over the Archipelago in Fig. 12) or all of the trajectories that required 4–6 days to transit from this region to Hudson Bay. Indeed, from Fig. 13b, elevated BrO appears to start to move from the Archipelago to central Hudson Bay starting about April 2–3. That the April 7 BrO appears less intense over the north western coast of Hudson Bay than on April 8 may be due to the presence of the low level clouds discussed earlier that blocked some of the DIAL (and GOME) observations as shown in Fig. 3.

Further evidence that the ODE was not initiated by triggering of BrO_x local to the Hudson Bay region follows from the application of the polar regional model described by Zeng et al. (2003, 2006). The model was run using BrO concentrations prescribed by the GOME TVCD distributed uniformly up to 300 m from the surface and thus cannot simulate the recycling of BrO_x. Figure 14a shows the prescribed TVCD and Fig. 14b the temporal change in the ozone mixing ratio from the model along the back-trajectories from central Hudson Bay for the period April 10–1. The model shows that although some low-ozone air from near Siberia may have contributed to the ODE observed over Hudson Bay, the majority of the contribution came from ozone destruction occurring over the Archipelago region. The model predicted the arrival of the ODE over Hudson Bay on April 4, likely a half to 1 day early since DIAL observed no ODE over the western portion of Hudson Bay on the flight to Thule in the morning of April 4, mentioned earlier. However, the simulated ozone mixing ratios over central Hudson Bay remained at ~1 ppbv through April 10 with ozone reaching to ~10 ppb briefly on April 5 and 6 due to mixing from above. Model sensitivity results (not shown) further indicate that low ozone mixing ratios remained over Hudson Bay even if local BrO in that region was removed (the prescribed BrO was arbitrarily set to zero in the model). In sum, the trajectories, GOME data, and the regional model of ozone change are consistent with halogen activation being triggered initially in the Archipelago and nearby Arctic Ocean region around March 30–April 1. From the GOME measurements, elevated BrO (and depleted ozone) was maintained in this air mass during transport over and around the islands of the Archipelago region and lowlands to Hudson Bay. Even if some exchange and mixing occurred with air of more normal O_3 content during the long-range transport, the continuous high tropospheric BrO illustrated by the GOME data would continue to efficiently destroy available O_3. It is possible that further halogen activation occurred from the underlying surface

Fig. 14 a The GOME specified TVCD along the 10-day back-trajectories from central Hudson Bay beginning on April 10. b The corresponding ozone mixing ratio along the back-trajectories from central Hudson Bay beginning on April 10
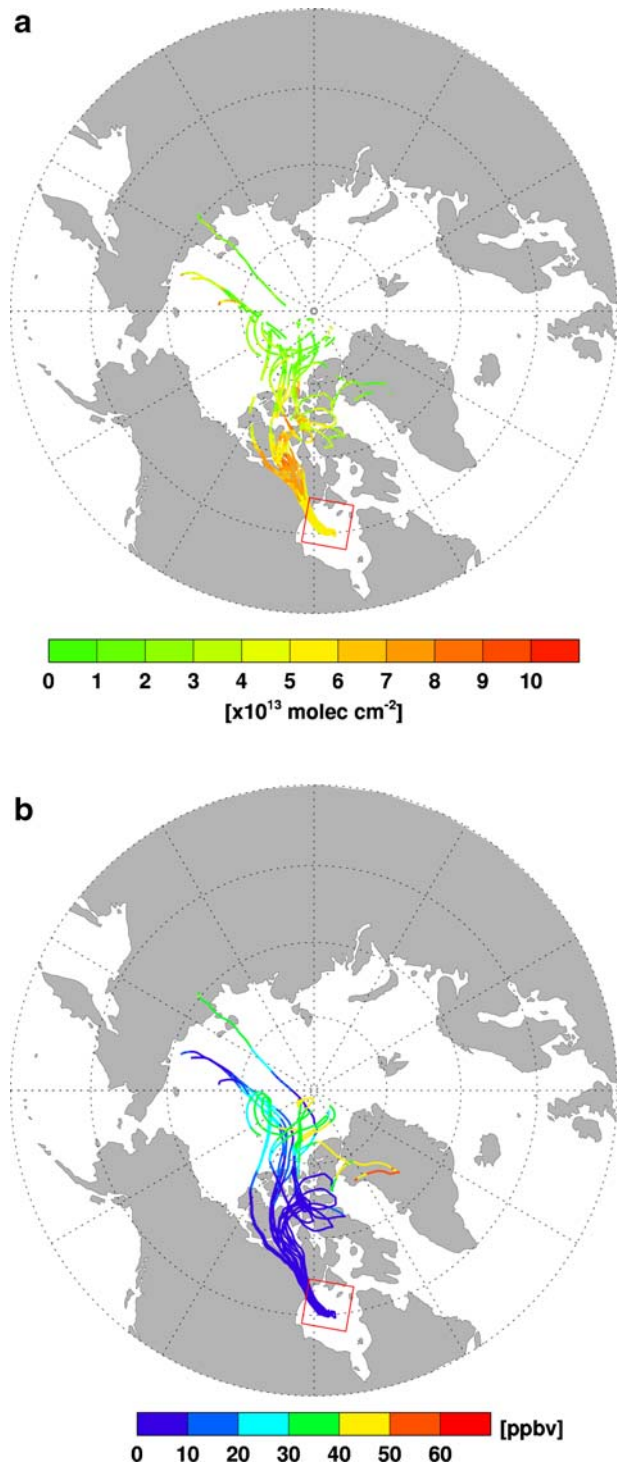
during transport to and upon the arrival of this air mass over Hudson Bay. However, with the large variation in the sea salt content and other chemical/physical properties of the surface snow/ice expected over this 1000–1500 km distance, the analysis suggests that deposition and subsequent recycling of constituents (e.g., HBr, HOBr, BrONO$_2$) formed during the initial period of the "bromine explosion" to/on the snow/ice surface or on aerosols dominated the maintenance of the high BrO$_x$ within the air mass during transport rather than sources from the local surface.

Figure 13 also shows that the change in the TVCD over Hudson Bay including areas several hundred kilometers to the northwest was surprisingly small and only about a factor of two from April 7–11. Although the aircraft sampled different air masses within the ODE on April 10 (central Hudson Bay) and April 11 (eastern Hudson Bay), ozone in the sampled surface layer changed by an order of magnitude: <1 ppbv on April 10 and ~10 ppbv on April 11. The BrO/Br ratio is given by:

$$[BrO]/[Br] \sim k_{Br/O3}[O_3]/\{J_{BrO} + k_{BrO/NO}[NO] + 2k_{BrO/BrO}[BrO]\} \qquad (8)$$

where the ks are the rate coefficients for the subscripted reactants (Platt and Janssen 1995; Tuckermann et al. 1997; Michalowski et al. 2000; Evans et al. 2003; Zeng et al. 2003). It is most sensitive to the concentration of O$_3$ and the first two terms in the denominator. For example, for constant BrO$_x$ and near noon solar conditions (near the local time of the satellite overpass on April 10), the ratio is expected to decrease by a factor of 35–40 if ozone was decreased from a normal mixing ratio of 40 ppbv to the average of 0.7 ppbv observed in the ODE on April 10. For the two portions of the ODE sampled on April 10 and April 11, where mean ozone was 0.7 and 9.7 ppbv, the expected change in the BrO/Br ratio would result in an increase in BrO by a factor of 4–5 provided BrO$_x$ was originally the same within the two air masses. Although the GOME resolution is only 320 km (E–W) × 40 km (N–S), it is comparable to the area of the flight track within the surface layer on April 10 and about twice that of the flight track of April 11. GOME shows an increase in the TVCD from April 10 to 11 but only by a factor of ~1.6. The much smaller than expected change in BrO requires that BrO$_x$ be much larger in the April 10 sampled surface layer compared to that on April 11. The implied strong variations of BrO$_x$ within the large scale ODE either reflect extreme heterogeneity of the source triggering and activation in the Archipelago region or that the mechanism outlined in the introduction is incomplete.

4 In situ observations of other constituents and a comparison of BrO mixing ratios within the ODE

We begin with a subset of the available in situ data from the April 10 flight. The local mid-time of the low level flight legs was 1330 LT (1830 UT) and the sky was clear: DIAL was obviously able to see the surface (Fig. 4) and the measured photolysis frequency of NO$_2$, J_{NO2}, was in the range of $1.4–1.6 \times 10^{-2}$ s^{-1}. Of course, measurements were not made within the air mass prior to activation of bromine radicals and subsequent ozone destruction. However, constituent observations within the ODE can be compared with mean and median values (Table 1) determined for all of the low altitude flight legs made north of 58°N during the TOPSE program in which no ozone depletion was observed.

Figure 15a shows the time series of soluble bromide for the flight starting near the first descent (D1 of Fig. 6). Soluble bromide includes any water-soluble constituent such as HBr, HOBr, BrONO$_2$, or aerosol Br$^-$ that is collected by the mist chamber technique (Scheuer et al.

Table 1 Surface layer mixing ratios north of 58° latitude, non-ODE samples

Constituent	Mean ± s.d.	Median
soluble bromide (pptv)	6.5±4.6	5
CO (ppbv)	151±11.5	154
Propane[a] (pptv)	606±110	581
ethyne[a] (pptv)	457±54	457
CH_3Br (pptv)	9.7±0.4	9.6
$CHBr_3$[a] (pptv)	1.41±0.8	1.1
NO_x (pptv)	9.4±7.7	9
Ozone (ppbv)	36.1±5.5	37.1

[a] These means and medians are from 52 samples taken between March 20 and April 10 rather than for all TOPSE flights because these hydrocarbons have a seasonal dependence easily seen over the February–May period (see Blake et al. 2003).

2003). Its substantial increase to 20–30 pptv within the ODE relative to the mean non-ODE mixing ratio of 6.5 pptv directly confirms current or past-active bromine chemistry.

CO data from two different instruments are also given in the figure to indicate the behavior of a long-lived "pollution" tracer. There was little change in CO with altitude and its mean mixing ratio of ~155 ppbv within the ODE was quite similar to non-ODE conditions (Table 1) indicating directly that the ODE was not related to a particular event of previous enhanced pollution. Other tracers of pollution events like NO_y or PAN were also not elevated within the ODE. Thus pollution input was not a necessary condition for the formation or maintenance of the ODE observed over Hudson Bay. There was no evidence that this ODE was associated with an air mass originating in Eurasia (cf., Bottenheim et al. 2002).

Figure 15b shows that propane (which has a large rate coefficient for reaction with Cl) and especially ethyne (which has large rate coefficients for reaction with Br and with Cl) were greatly reduced within the ODE compared to altitudes above the surface layer and compared to median non-ODE conditions (Table 1). This behavior has been observed routinely in previous studies (Jobson et al. 1994; Ramacher et al. 1999; Rudolph et al. 1999; Boudries and Bottenheim 2000) and Zeng et al. (2006) have presented a detailed analysis for the TOPSE flights. The magnitude of the reduction of ethyne and propane qualitatively confirms the presence of bromine and chlorine atoms and the inferred long age (~10 days) of the Hudson Bay ODE. It is also noted that the reduction in either hydrocarbon is less during the first low altitude leg, between 62,300 and 63,400 s, where O_3 was only partially depleted to a mean of 7.2 (±2.5) ppbv. The increases in O_3 and these two hydrocarbons in this partially depleted air mass are consistent with downward input and mixing of ~13% of local free tropospheric air with air deeper within the ODE where O_3 and hydrocarbons were significantly smaller. Lateral mixing on the northern edge of the ODE also could contribute to the increases in O_3 and hydrocarbons.

Figure 15c gives the time series of methyl bromide (CH_3Br, lifetime ~8 months) and bromoform ($CHBr_3$, lifetime ~1/2 month). Both constituents were elevated in the ODE relative to higher altitudes or to their means in low altitude non-depleted air (Table 1). Since both constituents have maritime sources (Sturges 1993), the increases observed in the depleted air suggest that the air mass was in contact with open seawater earlier in its history. The Archipelago region does contain a number of polynyas.

The behavior of NO_x (NO + NO_2) allows an estimate of the BrO concentration for comparison with that derived from the GOME observations. As shown in Fig. 16 the NO_x
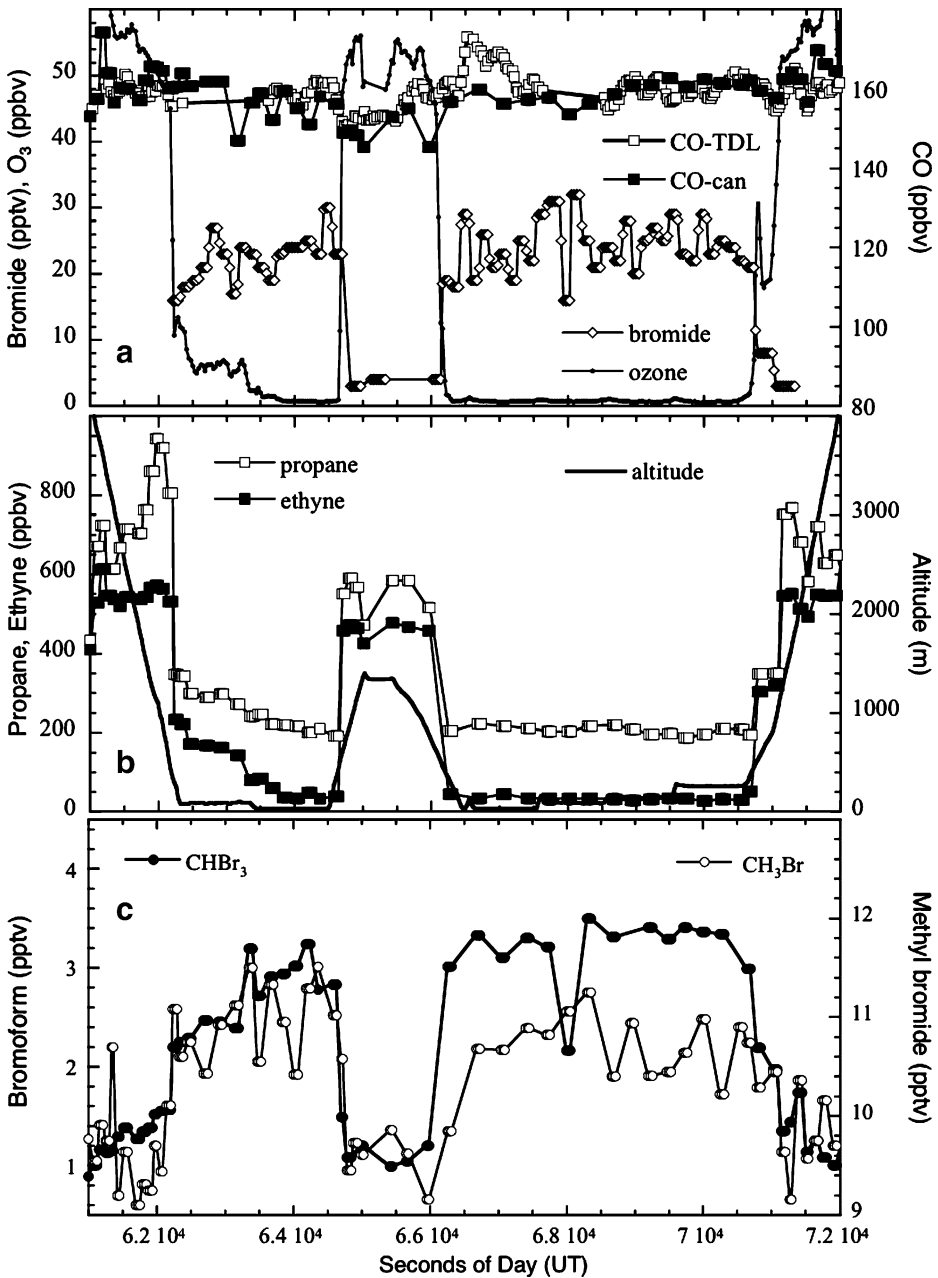
Fig. 15 **a** Time series of CO and soluble bromide from the April 10 flight. Ozone is repeated in the panel for ease of reference to the depleted ozone periods. The CO data are from a tunable diode laser system (M. Coffey, J. Hannigan, NCAR) and from can samples (Blake et al. 2003). The soluble bromide data are from the U. of New Hampshire group (Scheuer et al. 2003). **b** Time series of propane, ethyne and radar altitude. **c** Time series of bromoform and methyl bromide. Data for (**b**) and (**c**) from Blake et al. 2003. All the data in the three panels are from a 30-s merged file provided by L. Emmons, NCAR

and the NO/NO$_2$ ratio increased significantly as the aircraft flew from within the partially depleted air mass (6,220–63,160 s) where mean O$_3$ was 7.2 ppbv to within the central part of the ODE where O$_3$ averaged 0.74 ppbv (66,400–70,650 s). The increase in mean NO$_x$ of over a factor of three from 5.1 (±3.0) pptv to 17.3 (±4.8) pptv is attributed to the decrease in the rate of daytime formation of BrONO$_2$: for constant NO$_x$ and BrO$_x$, BrO and NO$_2$ should both decrease in favor of Br and NO, commensurate with the decrease in O$_3$ (Ridley and Orlando 2003; Evans et al. 2003; Ridley et al. 2003). Filtering the individual 10-s measurements of NO and NO$_2$ to mixing ratios = 3 pptv, the mean of individual NO/NO$_2$ ratio measurements increased from 1.5 (±1.2) to 2.4 (±1.1) (207 samples).

At steady-state, the NO/NO$_2$ ratio during daytime is given by

$$[NO]/[NO_2] = \left\{ \left(k_{NO/O3}[O_3] + k_{NO/RO2}[RO_2] + k_{NO/BRO}[BrO] \right) / J_{NO2} \right\}^{-1} \qquad (9)$$

where the ks are the rate coefficients for the subscripted reactants and RO$_2$ is the sum of peroxy radicals including HO$_2$. With no RO$_2$ or BrO radicals present, a mean air temperature of the low altitude legs of −22.5 C, and the mean measured J_{NO2} (1.5±0.3× 10^{-2} s^{-1}), Eq. 9 would give a ratio near 100 for the central part of the ODE and a ratio of 9.7 for the partially depleted air. Using the mean of the measured RO$_2$ in each air mass (Fig. 16), and assuming the absence of BrO, the ratio in the central ODE and in the partially depleted air would be 7.1 and 4.8, respectively, still significantly larger than observed. If all of the remaining disagreement in the ratio is attributed to BrO radicals then mixing ratios of 6 and 10 pptv would be required in the central ODE and in the partially depleted air, respectively. The requirement of larger BrO in the partially depleted air compared to the central ODE is qualitatively consistent with the expected decrease in the BrO/Br ratio as O$_3$ is depleted to very small values (Platt and Janssen 1995; Tuckermann et al. 1997). Because the individual mixing ratios of NO and NO$_2$ were small, the estimate of the average BrO abundance is accurate to within a factor of ~2.

Figure 13b shows the April 10 satellite pass over central Hudson Bay at ~1240 LT during the time of the aircraft flight. Using the TVCD = 5.5×10^{13} molec cm^{-2} and
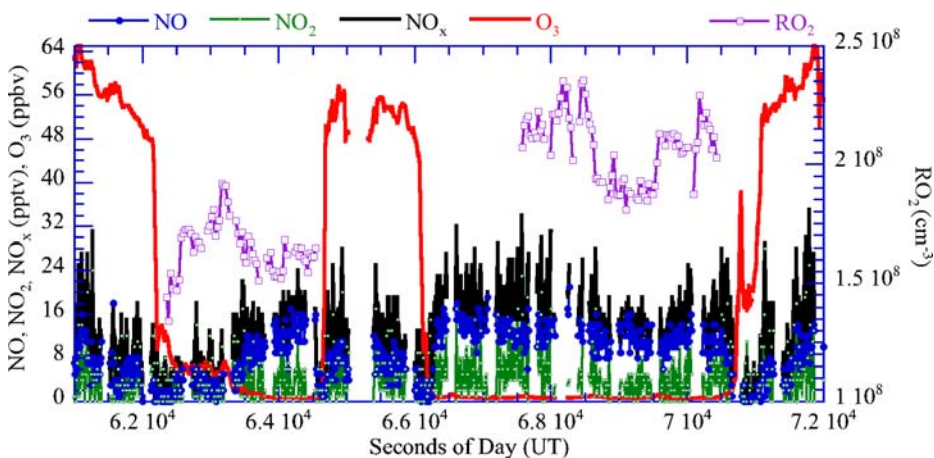

Fig. 16 Time series of NO, NO$_2$, NO$_x$, O$_3$ and total peroxy radicals (RO$_2$), which include HO$_2$. The active nitrogen and ozone data are averaged over 10 μs, and the RO$_2$ data over 30 s (Cantrell et al. 2003)

assuming that all of the BrO was contained below and uniformly distributed within the surface layer, which had an average depth of 465 m and an average temperature of −22.5 C, yields a BrO mixing ratio of 41 pptv with an uncertainty of ~40%. On April 11, a similar calculation gives 49 pptv. The April 10 value is at least two to three times larger than that derived from the NO/NO_2 ratio. Although the result from the ratio would suggest that the model runs of Section 3 used too high concentrations of BrO, and thus too rapid a depletion of O_3, the conclusion that the depletion was ultimately caused by triggering over the Archipelago would not be affected because a processing time of at least 9 days occurred before the air mass was investigated in detail over Hudson Bay on April 10.

Both the April 10 and 11 satellite values are also on the high side of most ground-based measurements of BrO for the Arctic where the maximum values reported are 30 pptv and are more often in the range of 5–15 pptv (Hausmann and Platt 1994; Tuckermann et al. 1997; Hönninger and Platt 2002; Avallone et al. 2003; Morin et al. 2005). An exception is the study by Hönninger (2002) who reported reasonable agreement between GOME retrievals and direct measurements of BrO by long-path Differential Optical Absorption Spectroscopy techniques at Kuujjuarapik (located on the southeast shore of Hudson Bay, see Fig. 1). Surface BrO measurements ranged up to a maximum of 30 ppt, with peak levels typically between 10 and 20 pptv associated with ozone depletion events. He assumed a stratospheric plus free tropospheric background of 4×10^{13} molec cm^{-2} and a surface layer depth of 1 km. Interestingly, the periods of low ozone/high BrO that he observed were also associated with air mass transport from the Archipelago region. The largest mixing ratio of BrO reported for the Arctic Ocean region is 63 pptv, but that value was also determined from a satellite total column measurement (Jacobi et al. 2006). The difference between the present GOME and in situ estimates is surely attributable to errors in the measured NO/NO_2 ratio and assumptions made to derive the TVCD. Assigning all of the BrO to the surface layer may also contribute to the high value determined from the TVCD since there are observations that indicate small but significant mixing ratios of BrO in the "free" troposphere (McElroy et al. 1999; Fitzenberger et al. 2000).

A similar comparison of the aircraft and GOME data cannot be made for April 11. On this flight, which started earlier in the morning at 0900 LT, the levels of NO_x within the partially depleted air mass over the Bay were essentially zero to within the accuracy of the measurements even considering that the snow surface can be a daytime source of NO_x and HONO (Honrath et al. 1999; Beine et al. 2002). Over two 15–20 min legs flown at 525 and 30 m altitude over the Bay, median and mean NO_x were 0 and −0.5 (±4.5) pptv. Formation of N_2O_5 especially, but also $BrONO_2$ and HNO_4, and deposition to the surface or aerosols during the ~10 h nighttime period for latitudes near Churchill is an effective nighttime sink for active nitrogen (e.g., Tie et al. 2003) at these latitudes compared to higher latitudes, e.g., the Archipelago region, that experience continuous sunlight in early April and where N_2O_5 formation would be insignificant. Indeed, it is important to recognize that the BrO_x activity in the ODE over Hudson Bay persisted despite the nighttime period. Formation of labile nighttime constituents like Br_2 and HOBr must have strongly dominated formation of HBr for the more than 1-week period that the ODE persisted over Hudson Bay. The very small ethyne mixing ratio in the ODE (Fig. 15b) is consistent with this requirement.

5 Summary

We conclude that the ODE that persisted from about April 5–15 did not result from BrO_x triggering and activation in the Hudson Bay region but was the result of long-range transport (1,000–1,500 km) after triggering over the Arctic Archipelago/Arctic Ocean

region of northern Canada. The back-trajectories, the GOME satellite data, and the regional modeling of O_3 confirm that a thin surface layer of low O_3 and high BrO could survive this transport over or around the rough terrain of this region. The high BrO activity was maintained as the air mass moved from a region of continuous sunlight to a region where ~10 h of darkness occurred daily. Some mixing with air of normal ozone content likely occurred during transport, but the BrO content revealed by GOME remained sufficient to maintain rapid net destruction of O_3.

Quantitatively, the BrO mixing ratio determined indirectly from the in situ mean NO/NO_2 ratio was at least a factor of 2–3 lower than was derived by assuming that all of the tropospheric column determined from the GOME observations was contained within the surface layer depth defined by the aircraft observations over Hudson Bay on April 10. The GOME data show that, once triggered over the Archipelago region, BrO remained enhanced for several weeks within the air mass. BrO_x recycling was maintained even though the surface changed from that of the Archipelago and ocean surface to that of the lowlands and snow/ice surface of Hudson Bay implying that local additional halogen input from the underlying surface was not the dominant source of the reactive bromine. In this case, the surface snow/ice/open ocean water of the Archipelago region was required for triggering the halogen chemistry, but our analysis argues that the reactive bromine initially produced could be maintained by recycling of constituents on the surface or on aerosols during the long-range transport. Evans et al. (2003) reached similar conclusions from their model study of TOPSE observations.

Transport of or production of aerosols in air masses could be important for the halogen chemical recycling. Frieß et al. (2004) have reported that their ground observations of enhanced BrO in the Antarctic were accompanied by increased aerosol scattering and that recycling was likely dominated by suspended surface area density. Gauchard et al. (2005) have also reported enhancements of larger particles (0.5–5 μm) associated with ozone (and mercury) depletion events at Kuujjuarapik (see Fig. 1), and they suggested that the particle enhancement was not from in situ formation, but rather from air mass transport.

Given the long duration of the Hudson Bay ODE, and the potential for aerosols to be deposited to the different surfaces during transport to and residence over Hudson Bay, it is surprising that the aerosol surface area density remained sufficiently large for the recycling to be maintained. The DIAL scattering ratio clearly showed enhanced particle concentrations and sulfate and soluble bromide were also enhanced within the ODE (Scheuer et al. 2003; Ridley et al. 2003). The surface layer was also near saturation relative to ice. Either the recycling by, for example, reaction (7) is largely independent of the type of acidic aerosol or the observations further imply that aerosol surface area was regenerated during transport and during the long residence time over Hudson Bay. Since there was no evidence of a pollution source of aerosols from the CO, NO_y and other gaseous tracers, there is indirect evidence that aerosols dominated by ice content are efficient for recycling (Barrie et al. 1988; Curry and Radke 1993). Support for ice crystal surface area dominating the recycling is that intense ODEs observed over Alert are frequently accompanied by high concentrations of ice particles (Bottenheim et al. 2002; Ridley and Orlando 2003). Zeng et al. (2006) have also shown that elevated BrO TVCDs anticorrelate with surface temperature, perhaps consistent with promotion of near-saturation and ice particle formation.

References

Arimoto, R., Zeng, T., Davis, D., Wang, Y., Khaing, H., Nesvit, C., Huey, G.: Concentrations and sources of aerosol ions and trace elements during ANTCI-2003. Atmos. Environ. (2007) doi:10.1016/j.atmosenv.2007.05.054

Atlas, E.L., Ridley, B.A., Cantrell, C.A.: The Troposphere Ozone Production about the Spring Equinox (TOPSE) Experiment: introduction. J. Geophys. Res. **108**(D4), 8353 (2003) doi:10.1029/2002JD003172

Avallone, L.M., Toohey, D.W., Fortin, T.J., McKinney, K.A., Fuentes, J.: In situ measurements of bromine oxide at two high-latitude boundary layer sites: Implications of variability. J. Geophys. Res. **108**(D3), 4089 (2003) doi:10.1029/2002JD002843

Barrie, L., Platt, U.: Arctic tropospheric chemistry: an overview. Tellus **49B**, 450–454 (1997)

Barrie, L.A., Bottenheim, J.W., Schnell, R.C., Crutzen, P.J., Rasmussen, R.A.: Ozone destruction and photochemical reactions at polar sunrise in the lower Arctic atmosphere. Nature **334**, 138–141 (1988)

Barrie, L.A., Platt, U., Shepson, P.: Surface ozone depletion at polar sunrise fueled by sea-salt halogens. IGACtivities Newsletter, International Global Atmospheric Chemistry Project 14, pp. 4–7, September (1998)

Beine, H.J., Dominé, F., Simpson, W., Honrath, R.E., Sparapani, R., Zhou, Z., King, M.: Snow-pile and chamber experiments during the Polar Sunrise Experiment 'Alert 2000': exploration of nitrogen chemistry. Atmos. Environ. **36**, 2707–2719 (2002)

Blake, N.J., et al.: The seasonal evolution of NMHCs and light alkyl nitrates at middle to high latitudes during TOPSE. J. Geophys. Res. **108**(D4), 8359 (2003) doi:10.1029/2001JD001467

Bottenheim, J.W., Gallant, A.C., Brice, K.A.: Measurements of NO_y species and O_3 at 82°N latitude. Geophys. Res. Lett. **13**, 113–116 (1986)

Bottenheim, J.W., Fuentes, J.D., Tarasick, D.W., Anlauf, K.G.: Ozone in the Arctic lower troposphere during winter and spring 2000 (ALERT2000). Atmos. Environ. **36**, 2535–2544 (2002)

Boudries, H., Bottenheim, J.W.: Cl and Br atom concentrations during a surface boundary layer ozone depletion event in the Canadian high Arctic. Geophys. Res. Lett. **27**, 517–520 (2000)

Browell, E.V., et al.: Ozone, aerosol, potential vorticity, and trace gas trends observed at high-latitudes over North America from February to May 2000. J. Geophys. Res. **108**(D4), 8369 (2003) doi:10.1029/2001JD001390

Cantrell, C.A., Edwards, G.D., Stephens, S. Mauldin, L., Kosciuch, E., Zondlo, M., Eisele, F.: Peroxy radical observations using chemical ionization mass spectrometry during TOPSE. J. Geophys. Res. **108**(D6), 8371 (2003) doi:10.1029/2002JD002715

Curry, J.A., Radke, L.F.: Possible role of ice crystals in ozone destruction of the lower Arctic atmosphere. Atmos. Environ. **27A**, 2873–2879 (1993)

Domine, F., Taillandier, A.S., Simpson, W.R., Severin, K.: Specific surface area, density and microstructure of frost flowers. Geophys. Res. Lett. **32**, L13502 (2005) doi:10.1029/2005GL023245

Evans, M.J., et al.: Coupled evolution of BrO_x–ClO_x–HO_x–NO_x chemistry during bromine-catalyzed ozone depletion events in the arctic boundary layer. J. Geophys. Res. **108**(D4), 8368 (2003) doi:10.1029/2002JD002732

Fan, S.-M., Jacob, D.J.: Surface ozone depletion in Arctic spring sustained by bromine reactions on aerosols. Nature **359**, 522–524 (1992)

Fitzenberger, R., Bösch, H., Camy-Peyret, C., Chipperfield, M.P., Harder, H., Platt, U., Sinnhuber, B.-M., Wagner, T., Pfeilsticker, K.: First profile measurements of tropospheric BrO. Geophys. Res. Lett. **27**, 2921–2924 (2000)

Foster, K.L., Plastridge, R.A., Bottenheim, J.W., Shepson, P.B., Finlayson-Pitts, B.J., Spicer, C.W.: The role of Br_2 and BrCl in surface ozone destruction at polar sunrise. Science **291**, 471–474 (2001)

Frieß, U., Hollwedel, J., König-Langlo, G., Wagner, T., Platt, U.: Dynamics and chemistry of tropospheric bromine explosion events in the Antarctic coastal region. J. Geophys. Res. **109** (D6) D06305 (2004) doi:10.1029/2003JD00413

Fuelberg, H.E., et al.: TRACE – a trajectory intercomparison. 2. Isentropic and kinematic methods. J. Geophys. Res. **101**, 23927–23939 (1996)

Gauchard, P.-A., Ferrari, C.P., Dommergue, A., Poissant, L., Pilote, M., Guehenneux, G., Boutron, C.F., Baussand, P.: Atmospheric particle evolution during a nighttime atmospheric mercury depletion event in the sub-Arctic at Kuujjuarapik/Whapmagoostui, Quebec, Canada. Sci. Total Environ. **336**, 215–224 (2005)

Hanson, D.R., Ravishankara, A.R.: Heterogeneous chemistry of bromine species in sulfuric acid under stratospheric conditions. Geophys. Res. Lett. **22**, 385–388 (1995)

Hausmann, M., Platt, U.: Spectroscopic measurement of bromine oxide in the high Arctic during Polar Sunrise Experiment 1992. J. Geophys. Res. **99**, 25399–25413 (1994)

Hönninger, G.: Halogen oxide studies in the boundary layer my multi-axis Differential Optical Absorption Spectroscopy and Active Longpath – DOAS, Ph. D., pp. 262. Thesis, University of Heidelberg, Germany (2002)

Hönninger, G., Platt, U.: Observations of BrO and its vertical distribution during surface ozone depletion at Alert. Atmos. Environ. **36**, 2481–2489 (2002)

Honrath, R.E., Peterson, M.C., Guo, S., Dibb, J.E., Shepson, P.B., Campbell, B.: Evidence of NO_x production within or upon ice particles in the Greenland snowpack. Geophys. Res. Lett. **26**, 695–698 (1999)

Jacobi, H.-W., Kaleschke, L., Richter, A., Rozanov, A., Burrows, J.P.: Observation of a fast ozone loss in the marginal ice zone of the Arctic Ocean. J. Geophys. Res. **111**, D15309 (2006) doi:10.1029/2005JD006715

Jobson, B.T., Niki, H., Yokouchi, Y., Bottenheim, J., Hopper, F., Leaitch, R.: Measurements of C_2–C_6 hydrocarbons during the 1992 Polar Sunrise Experiment: Evidence of Cl-atom and Br-atom chemistry. J. Geophys. Res. **99**, 25355–25368 (1994)

Kaleschke, L., Richter, A., Burrows, J., Afe, O., Heygster, G., Notholt, J., Rankin, A.M., Roscoe, H.K., Hollwedel, J., Wagner, T., Jacobi, H.-W.: Frost flowers on sea ice as a source of sea salt and their influence on tropospheric halogen chemistry. Geophys. Res. Lett. **31**, L16114 (2004) doi:10.1029/2004GL020655

Kalnajs, L.E., Avallone, L.M.: Frost flower influence on springtime boundary-layer ozone depletion events and atmospheric bromine levels. Geophys. Res. Lett. **33**, L10810 (2006) doi:10.1029/2006GL025809

Leaitch, W.R., Barrie, L.A., Bottenheim, J.W., Li, S.M.: Airborne observations related to ozone depletion at polar sunrise. J. Geophys. Res. **99**, 25499–25518 (1994)

Le Bras, G., Platt, U.: A possible mechanism for combined chlorine and bromine catalyzed destruction of tropospheric ozone in the Arctic. Geophys. Res. Lett. **22**, 599–602 (1995)

McConnell, J.C., Henderson, G.S., Barrie, L.A., Bottenheim, J., Niki, H., Langford, C.H.: Templeton, E.M.: Photochemical bromine production implicated in Arctic boundary-layer ozone depletion. Nature **355**, 150–152 (1992)

McElroy, C.T., McLinden, C.A., McConnell, J.C.: Evidence for bromine monoxide in the free troposphere during the Arctic Polar Sunrise. Nature **397**, 338–341 (1999)

Michalowski, B.A., Francisco, J.S., Li, S.-M., Barrie, L.A., Bottenheim, J.W., Shepson, P.B.: A computer model study of multiphase chemistry in the Arctic boundary layer during polar sunrise. J. Geophys. Res. **105**, 15131–15145 (2000)

Morin, S., Hönninger, G., Staebler, R.M., Bottenheim, J.W.: A high time resolution study of boundary layer ozone chemistry and dynamics over the Arctic Ocean near Alert, Nunavut. Geophys. Res. Lett. **32**, L08809 (2005) doi:10.1029/2004GL022098

Oltmans, S.J., Komhyr, W.D.: Surface ozone distributions and variations from 1973–1984 measurements at the NOAA Geophysical Monitoring for Climatic Change baseline observatories. J. Geophys. Res. **91**, 5229–5236 (1986)

Platt, U., Janssen, C.: Observation and role of the free radicals NO_3, ClO, BrO and IO in the troposphere. Faraday Disc. **100**, 175–198 (1995)

Platt, U., Lehrer, E.: Arctic troposphere halogen chemistry. Final Report to the European Community, ARCTOC, EVSV-CT93-0318 (1997)

Platt, U., Moortgat, G.K.: Heterogeneous and homogeneous chemistry of reactive halogen compounds in the lower troposphere. J. Atmos. Chem. **34**, 1–8 (1999)

Ramacher, B., Rudolph, J., Koppmann, R.: Hydrocarbon measurements during tropospheric ozone depletion events: Evidence for halogen atom chemistry. J. Geophys. Res. **104**, 3633–3653 (1999)

Rankin, A.M., Wolff, E.W., Martin, S.: Frost flowers – implications for tropospheric chemistry and ice core interpretation. J. Geophys. Res. **107** (D23), 4683 (2002) doi:10.1029/2002JD002492

Richter, A., Wittrock, F., Eisinger, M., Burrows, J.P.: GOME observations of tropospheric BrO in Northern Hemisphere spring and summer 1997. Geophys. Res. Lett. **25**, 2683–2686 (1998)

Ridley, B.A., Orlando, J.J.: Active nitrogen in surface ozone depletion events at Alert during spring 1998. J. Atmos. Chem. **44**, 1–22 (2003)

Ridley, B.A., et al.: Ozone depletion events observed in the high latitude surface layer during the TOPSE aircraft program. J. Geophys. Res. **108**(D4), 8356 (2003) doi:10.1029/2001JD001507

Rudolph, J., Fu, B.R., Thompson, A., Anlauf, K., Bottenheim, J.: Halogen atom concentrations in the Arctic troposphere derived from hydrocarbon measurements: Impact on the budget of formaldehyde. Geophys. Res. Lett. **26**, 2941–2944 (1999)

Sander, R., Burrows, J., Kaleschke, L.: Carbonate precipitation in brine – a potential trigger for tropospheric ozone depletion events. Atmos. Chem. Phys. **6**, 4653–4658 (2006)

Scheuer, E., Talbot, R.W., Dibb, J.E., Seid, G.K., DeBell, L., Lefer, B.: Seasonal distributions of fine aerosol sulfate in the North American Arctic basin during TOPSE. J. Geophys. Res. **108**(D4), 8370 (2003) doi:10.1029/2001JD001364

Simpson, W.R., Alvarez-Aviles, L., Douglas, T.A., Sturm, M., Domine, F.: Halogens in the coastal snow pack near Barrow, Alaska: evidence for active bromine air-snow chemistry during springtime. Geophys. Res. Lett. **32**, L04811 (2005) doi:10.1029/2004GL021748

Simpson, W.R., Carlson, D., Hoenninger, G., Douglas, T.A., Sturm, M., Perovich, D., Platt, U.: First-year sea-ice contact predicts bromine oxide (BrO) levels better than frost flower contact. Atmos. Chem. Phys. Discuss. **6**, 11051–11066 (2006)

Spicer, C.W., Plastridge, R.A., Foster, K.L., Finlayson-Pitts, B.J., Bottenheim, J.W., Grannas, A.M., Shepson, P.B.: Molecular halogens before and during ozone depletion events in the Arctic at polar sunrise: concentration and sources. Atmos. Environ. **36**, 2721–2731 (2002)

Sturges, W.T.: Halocarbons in the Arctic and Antarctic atmosphere. In: Niki, H., Becker, K. H. (eds.) The Tropospheric Chemistry in the Polar Regions. pp. 117–130, Springer-Verlag, New York (1993)

Sumner, A.L., Shepson, P.B.: Snowpack production of formaldehyde and its effect on the Arctic troposphere. Nature **398**, 230–233 (1999)

Tang, T., McConnell, J.C.: Autocatalytic release of bromine from Arctic snow pack during polar sunrise. Geophys. Res. Lett. **23**, 2633–2636 (1996)

Tie, X., et al.: Effect of sulfate aerosol on tropospheric NO_x and ozone budgets: model simulations and TOPSE evidence. J. Geophys. Res. **108**(D4), 8364 (2003) doi:10.1029/2001JD001508

Tuckermann, M., Ackermann, R., Gölz, C., Lorenzen-Schmidt, H., Seine, T., Stutz, J., Trost, B., Unold, W., Platt, U.: DOAS – observation of halogen radical-catalysed Arctic boundary layer ozone destruction during the ARCTOC-campaigns 1995 and 1996 in Ny-Ålesund, Spitsbergen. Tellus **49B**, 533–555 (1997)

Wagner, T., Platt, U.: Satellite mapping of enhanced BrO concentrations in the troposphere. Nature **395**, 486–490 (1998)

Wagner, T., Leue, C., Wenig, M., Pfeilsticker, K., Platt, U.: Spatial and temporal distribution of enhanced boundary layer BrO concentrations measured by the GOME instrument aboard ERS-2. J. Geophys. Res. **106**, 24225–24235 (2001)

Wang, X., Key, J.R.: Arctic surface, cloud, and radiation properties based on the AVHRR polar pathfinder dataset. Part I: Spatial and temporal characteristics. J. Climate **18**, 2558–2574 (2005)

Zeng, T., Wang, Y., Chance, K., Browell, E.V., Ridley, B.A., Atlas, E.L.: Widespread persistent near-surface ozone depletion at northern high latitudes in spring. Geophys. Res. Lett. **30**(24), 2298 (2003) doi:10.1029/2003GL018587

Zeng, T., Wang, Y., Chance, K., Blake, N., Blake, D., Ridley, B.: Halogen-driven low altitude O_3 and hydrocarbon losses in spring at northern high latitudes. J. Geophys. Res. **111**, D17313 (2006) doi:10.1029/2005JD006706